Title: Magnetically Guided Bi_2S_3@C/Fe_3O_4 Nanoparticles for Enhanced Photothermal-Radiation Synergy in Glioblastoma Treatment

Supplementary Information:

Experimental section:

Cy5.5-labeled Bi2S3@C/Fe3O4 NPs

Amino modification of Bi_2S_3@C/Fe_3O_4 nanoparticles: First, Bi_2S_3@C/Fe_3O_4 nanoparticles were dispersed in an ethanol/water mixed solution (volume ratio 1:1). 3-Aminopropyltriethoxysilane (APTES) was added to the dispersion at a concentration of 0.5 wt%, and the mixture was stirred at 60°C for 2–4 hours. This step introduced amino (-NH_2) groups onto the surface of the nanoparticles, providing reactive sites for subsequent dye conjugation. Conjugation of Cy5.5-NHS ester to amino-modified nanoparticles: The amino-modified Bi_2S_3@C/Fe_3O_4 nanoparticles were dispersed in PBS buffer (pH 7.4) at a concentration of 5 mg/mL and ultrasonicated for 10 minutes to prevent aggregation. Cy5.5-NHS ester (dissolved in a small volume of DMSO) was then added to the dispersion at a molar ratio of 1:10 (Cy5.5-NHS ester : nanoparticles). The mixture was shaken at room temperature for 2 hours in the dark, allowing the NHS ester group of Cy5.5 to react with the amino groups on the nanoparticles and form stable amide bonds. Purification of labeled nanoparticles: Unreacted Cy5.5-NHS ester was removed by dialysis using a dialysis bag with a molecular weight cutoff of 10 kDa, ensuring only Cy5.5-covalently labeled Bi_2S_3@C/Fe_3O_4 nanoparticles were retained for subsequent in vivo imaging experiments.

Magnetic targeted helmet production

Thin-layer CT scan was performed on the brain of mouse, and the helmet shape was designed for mouse according to the 3D reconstruction data of CT scan. Resin mouse helmet was constructed using 3D printing technology, and a NdFeB magnet (diameter: 7 mm, height: 2 mm) was placed on the top of the helmet. The mouse wore helmet for 12 h after each injection.

Histopathological evaluation of organ tissues

After 14 days of treatment, the mice were sacrificed and main organ tissues (heart, liver,

spleen, lung, and kidney) were collected for pathology analysis using the same tissue dissection process, and later subjected to hematoxylin and eosin (H&E) staining.

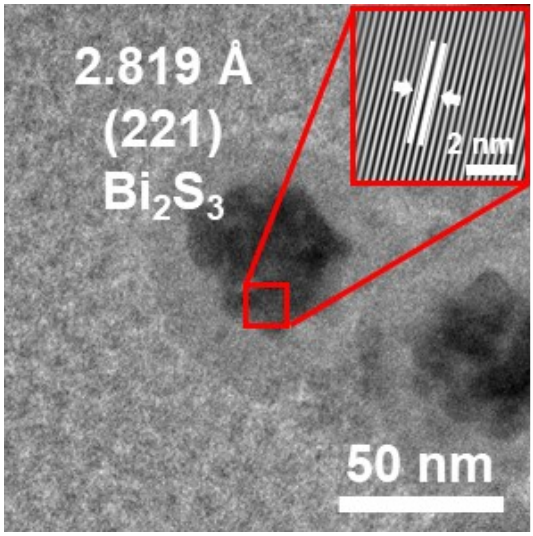

Figure S1. HR-TEM image of Bi_2S_3@C/Fe_3O_4 NPs.

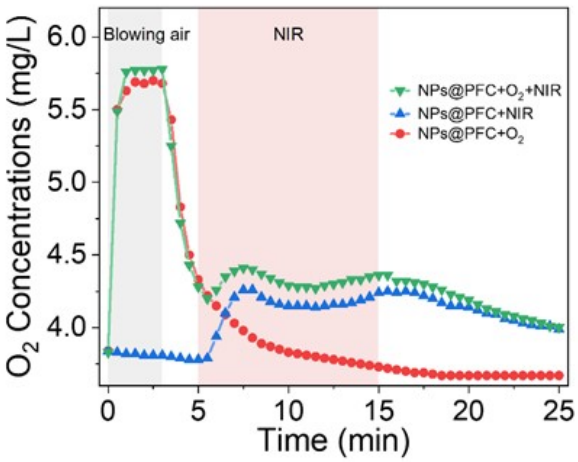

Figure S2. Oxygen storage performance of Bi_2S_3@C/Fe_3O_4 NPs.

Hypoxia is a hallmark of solid tumors[1, 2], significantly enhancing cancer cells' resistance to therapeutic interventions. This underscores the critical importance of adequate oxygenation in radiation therapy (RT) and radiotherapy (PTT). Liquid perfluorocarbon (PFC) possesses the unique ability to dissolve substantial amounts of oxygen and function as efficient oxygen carriers, making them suitable candidates for blood substitutes[3, 4, 5]. Near-infrared (NIR) light can induce rapid release of dissolved oxygen, leading to immediate oxidation, which is crucial for overcoming hypoxia-induced resistance to RT[6, 7, 8]. The yolk-shell structure of Bi_2S_3@C/Fe_3O_4 NPs allows for effective PFC loading. Given that Bi_2S_3@C/Fe_3O_4 NPs have been validated as effective photothermal agents, they generate heat under NIR laser irradiation, thereby increasing the temperature and promoting the release of oxygen from the PFC-loaded NPs.

Upon adding NPs@PFC+O_2 to deoxygenated water and irradiating the solution with an NIR laser, we observed a significant increase in oxygen concentration in real-time, as depicted in Figure S2. In contrast, the oxygen concentration decreased gradually in the absence of laser exposure. Unlike the open system used in these experiments, actual tumors represent a relatively closed environment, where the oxygen released by NPs@PFC+O_2 may persist longer, enhancing tumor oxygenation and providing novel strategies for improving the hypoxic tumor microenvironment.

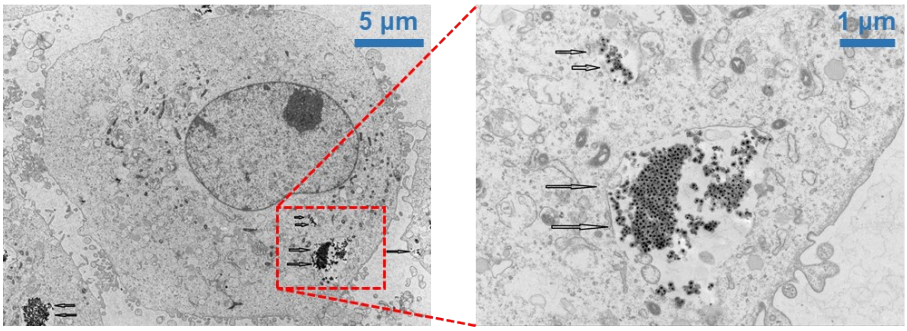

Figure S3. TEM images of Bi_2S_3@C/Fe_3O_4 NPs endocytosed by U87MG-Luc cells after 6 h.

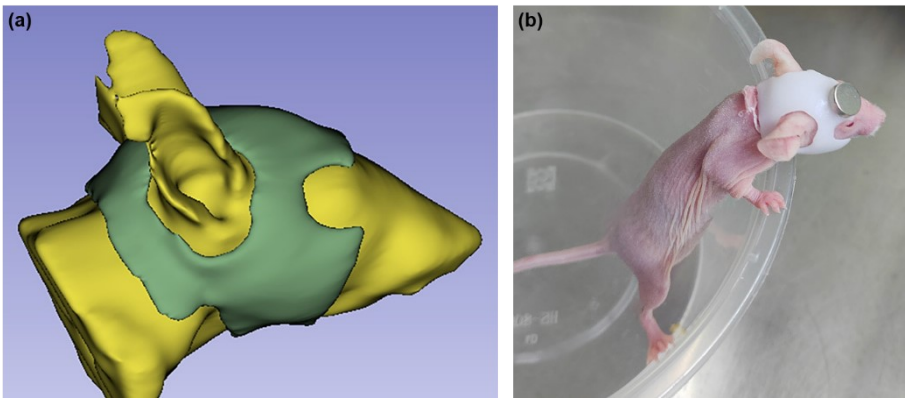

Figure S4. (a) Model diagram and (b) physical image of the mouse magnetic helmet.

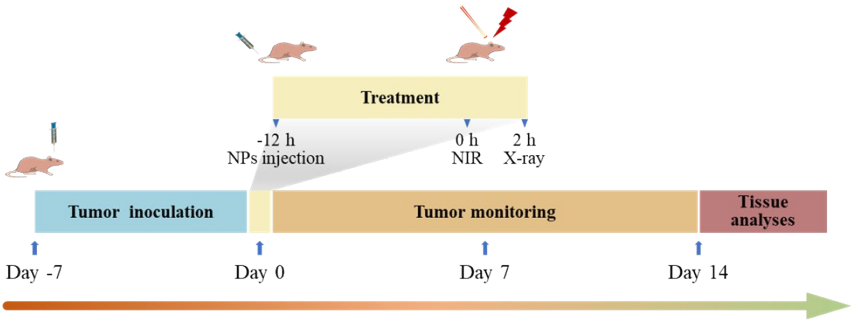

Figure S5. Schematic diagram of photothermal therapy and radiotherapy for U87MG-Luc tumor-bearing mice.

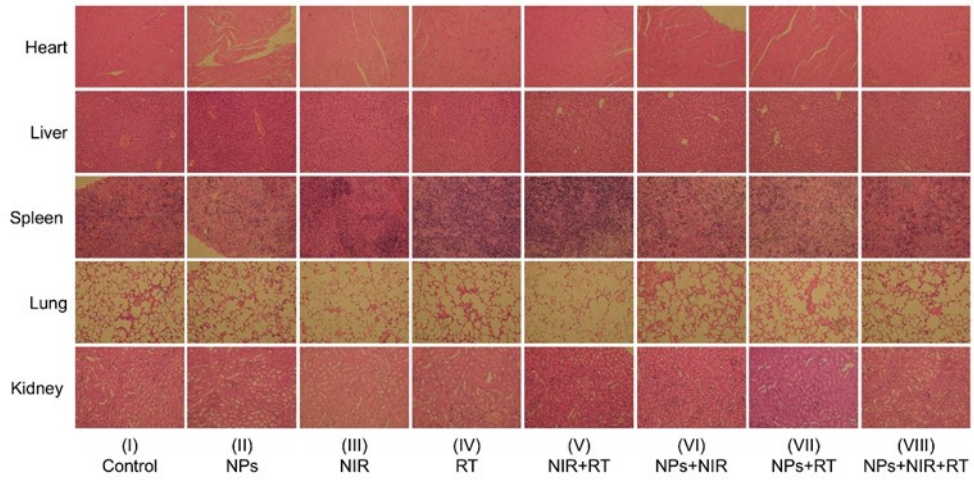

Figure S6. H&E assay images of major organs from each group after 14 days of treatment.

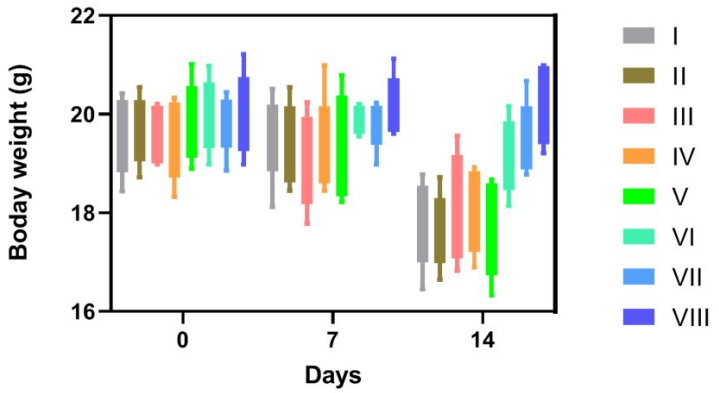

Figure S7. The changes of mouse body weight post received various treatments.

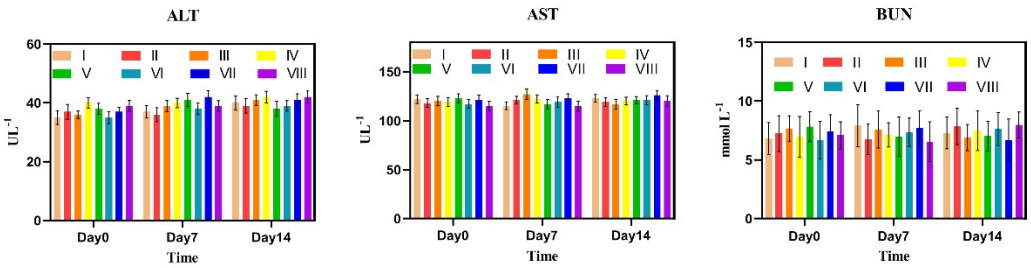

Figure S8. Serum levels of alanine aminotransferase (ALT), aspartate aminotransferase (AST), and blood urea nitrogen (BUN) in mice during the treatment process.

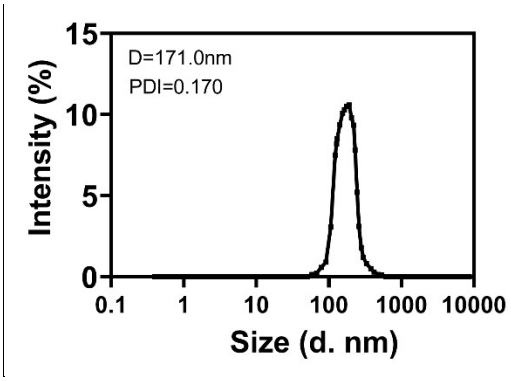

Figure S9. Dynamic light scattering analysis of the nanoparticles, showing the intensity-weighted hydrodynamic diameter (D=171.0nm) and polydispersity index (PDI = 0.170), which indicates excellent dispersion and stability.

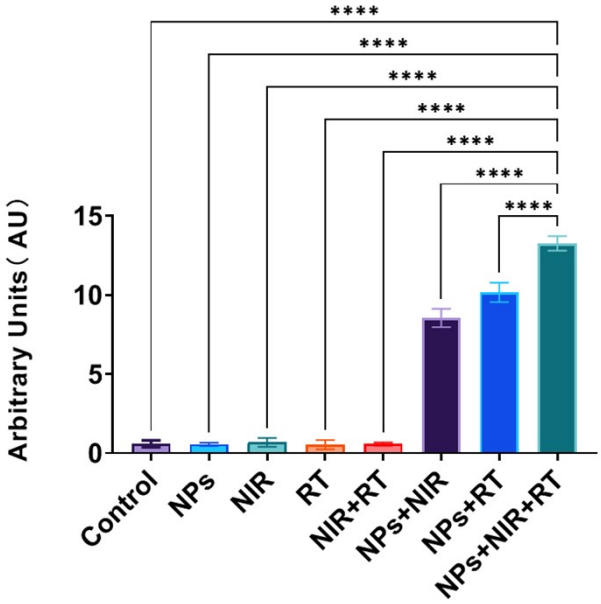

Figure S10. Quantitative analysis of DNA damage in different treatment groups.

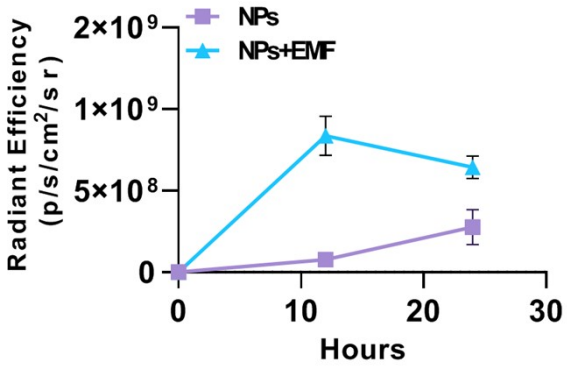

Figure S11. Quantitative analysis of fluorescence intensity in the intracranial region of

U87MG-Luc tumor-bearing mice injected with Cy5.5-labeled Bi_2S_3@C/Fe_3O_4 NPs.

References:

1. Vaupel P, Kallinowski F, Okunieff P. Blood flow, oxygen and nutrient supply, and metabolic microenvironment of human tumors: a review. Cancer research. 1989;49:6449-65. Epub 1989/12/01.
2. Horsman MR, Vaupel P. Pathophysiological Basis for the Formation of the Tumor Microenvironment. Front Oncol. 2016;6:66. Epub 2016/05/06.
3. Nocentini G, MacLaren G, Bartlett R, De Luca D, Perdichizzi S, Stoppa F, Marano M, Cecchetti C, Biasucci DG, Polito A, AlGhobaishi A, Guner Y, Gowda SH, Hirschl RB, Di Nardo M. Perfluorocarbons in Research and Clinical Practice: A Narrative Review. Asaio j. 2023;69:1039-48. Epub 2023/08/08.
4. Cabrales P, Carlos Briceño J. Delaying blood transfusion in experimental acute anemia with a perfluorocarbon emulsion. Anesthesiology. 2011;114:901-11. Epub 2011/02/18.
5. Krafft MP. Alleviating tumor hypoxia with perfluorocarbon-based oxygen carriers. Curr Opin Pharmacol. 2020;53:117-25. Epub 2020/09/27.
6. Song G, Liang C, Yi X, Zhao Q, Cheng L, Yang K, Liu Z. Perfluorocarbon-Loaded Hollow Bi2Se3 Nanoparticles for Timely Supply of Oxygen under Near-Infrared Light to Enhance the Radiotherapy of Cancer. Adv Mater. 2016;28:2716-23. Epub 2016/02/06.
7. Yang J, Xie R, Feng L, Liu B, Lv R, Li C, Gai S, He F, Yang P, Lin J. Hyperthermia and Controllable Free Radical Coenhanced Synergistic Therapy in Hypoxia Enabled by Near-Infrared-II Light Irradiation. ACS Nano. 2019;13:13144-60. Epub 2019/10/15.
8. Seah GL, Yu JH, Koo BI, Lee DJ, Nam YS. Cancer-targeted reactive oxygen species-degradable polymer nanoparticles for near infrared light-induced drug release. J Mater Chem B. 2018;6:7737-49. Epub 2018/12/14.